



Aalborg Universitet

**AALBORG UNIVERSITY**  
DENMARK

## **Distribution of Defects in Wind Turbine Blades and Reliability Assessment of Blades Containing Defects**

Toft, Henrik Stensgaard; Branner, Kim; Berring, Peter; Sørensen, John Dalsgaard

*Published in:*  
EWEC 2009 Marseille

*Publication date:*  
2009

*Document Version*  
Publisher's PDF, also known as Version of record

[Link to publication from Aalborg University](#)

### *Citation for published version (APA):*

Toft, H. S., Branner, K., Berring, P., & Sørensen, J. D. (2009). Distribution of Defects in Wind Turbine Blades and Reliability Assessment of Blades Containing Defects. In *EWEC 2009 Marseille: Europe's premier wind energy event, Parc Channot, Marseille, France 16-19 March 2009* The European Wind Energy Association.

### **General rights**

Copyright and moral rights for the publications made accessible in the public portal are retained by the authors and/or other copyright owners and it is a condition of accessing publications that users recognise and abide by the legal requirements associated with these rights.

- Users may download and print one copy of any publication from the public portal for the purpose of private study or research.
- You may not further distribute the material or use it for any profit-making activity or commercial gain
- You may freely distribute the URL identifying the publication in the public portal -

### **Take down policy**

If you believe that this document breaches copyright please contact us at [vbn@aub.aau.dk](mailto:vbn@aub.aau.dk) providing details, and we will remove access to the work immediately and investigate your claim.

# Distribution of Defects in Wind Turbine Blades and Reliability Assessment of Blades Containing Defects

Henrik Stensgaard Toft  
Aalborg University  
Denmark  
[hst@civil.aau.dk](mailto:hst@civil.aau.dk)

Kim Branner  
Risø-DTU  
Denmark  
[kim.branner@risoe.dk](mailto:kim.branner@risoe.dk)

Peter Berring  
Risø-DTU  
Denmark  
[peter.berring@risoe.dk](mailto:peter.berring@risoe.dk)

John Dalsgaard Sørensen  
Aalborg University & Risø-DTU  
Denmark  
[jds@civil.aau.dk](mailto:jds@civil.aau.dk)

## Abstract

In the present paper two stochastic models for the distribution of defects in wind turbine blades are proposed. The first model assumes that the individual defects are completely randomly distributed in the blade. The second model assumes that the defects occur in clusters of different size based on the assumption that one error in the production process tends to trigger several defects. For both models additional information about number, type and size of the defects is included as stochastic variables.

The probability of failure for a wind turbine blade will not only depend on variations in the material properties and the load but also on potential defects in the blades. As a numerical example the probability of failure is calculated for the main spar both with and without defects in terms of delaminations. The delaminations increase the probability of failure compared to a perfect blade, but by applying Non Destructive Inspection (NDI) techniques after production the probability of failure can be updated.

## 1 Introduction

Calculation of the load carrying capacity for wind turbine blades has been widely studied during the last decades leading to more refined FE calculations and failure criteria. But there still seems to be a variation in the load carrying capacity which to some extent can be caused by physical variations in the material properties. However, local production defects in the blades which are due to minor or gross variations in the manufacturing process can also influence the load carrying capacity. During operation in-service damage from cyclic

and ultimate loading of the blade also influence the capacity.

The influence of variations in the material properties has been studied in [1] where also different methods for determination of the probability of failure for wind turbine blades are considered.

For production defects the load carrying capacity is mainly influenced by the following parameters [2]:

- Type of defect
- Size of defect
- Position of defect

The influence of these three parameters on the load carrying capacity in some discrete cases has been studied in the research project SaNDI which focuses on sandwich structures for ships, see [3], [4] and [5]. The type of defect is important because not all failure modes are influenced by a particular type of defect. The size affects the amount of strength reduction and the position determines the critical loading and failure modes.

The production defects can also influence the fatigue properties of the blade because defects can lead to stress concentrations in the material. The stress concentrations can lead to additional crack initiation during service or growth of the individual defects. In order to secure that the local defects and in-service damage do not lead to failure of the blade during operation, a damage tolerant approach is often adapted during blade design. [6] has proposed a method for damage assessment of damage tolerant structures.

In normal blade design the influence of variations in the material properties is taken into account by reducing the material properties to a characteristic value (typical 5% quantile) and applying a partial safety factor [7] and [8]. In order to avoid defects from the production process in the wind turbine blade quality control by Non Destructive Inspection (NDI) such as visual inspection or ultrasound scanning is performed after production [6]. However, the NDI is not perfect and remaining uncertainty due to production defects is assumed to be captured by the partial safety factor on the material properties.

NDI is in practical blade manufacturing in many cases followed up by destructive inspection and repair. Such destructive inspection is used as a measure to better quantify type and size of the defect before determining the extent of the repair as well as a basis for calibration and control of the NDI. In the following we will not go into details with possible destructive follow up on NDI.

In the present paper two stochastic models for the distribution of defects in wind turbine blades are proposed. The models introduce the position of the defects as well as additional information about the defect such as number, type and size in a stochastic manner.

The ability of the NDI to identify defects in the wind turbine blade is modelled by Probability of Detection (PoD) curves and the distribution of the defect size can be updated based on Bayesian methods.

The influence of the production defects on the ultimate load carrying capacity for the blade is calculated for a few selected defects and compared to the capacity of a blade not containing any defects. The influence of the most important material properties is also investigated by sensitivity analysis. Based on the calculated load carrying capacities the reliability of the blade is calculated and the influence of NDI is investigated.

The strength models and the defect descriptions in the paper are set up on an empirical basis and have not yet been calibrated against observations from blade manufacturing and testing.

## 2 Production Defects

Production defects for wind turbine blades are typically [6]:

- Delaminations
- Wrinkles
- Matrix cracks
- Voids
- Defects in glued joints

In the present paper only delaminations are taken into account. However, the approach taken is general and additional types of defects can be included in the model.

Delaminations are areas of poor or no bonding between adjacent plies which can be caused by air traps, a poor infusion of resin in the given area or similar dependent of the production process. For prepreg the delaminations can also be due to a poor consolidation during curing. The delaminations will mainly reduce the compression strength of the wind turbine blade because of out-of-plane buckling [9]. If the delamination is placed near the outer or inner surface of the laminate the delamination induces local buckling of a group of plies, see figure 1. If the delamination is placed near the centre of the material the strength reduction will be caused by global buckling of the laminate, see figure 1 [10]. In fatigue loading the delamination can lead to a stress concentration which can lead to delamination growth and significantly reduce the fatigue life for the blade.

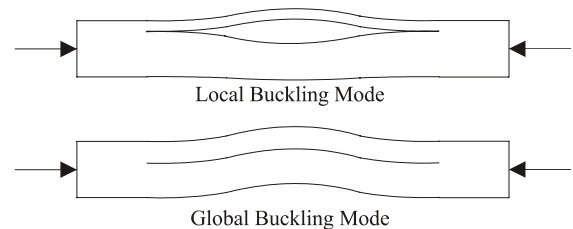


**Figure 1:** Local and global buckling mode for delamination.

The influence of delaminations on the ultimate compression strength has been studied in [10] for GFP and in [3] and [4] for sandwich structures exposed to different load cases. The main parameters which influence the strength reduction are the size of the delamination and the through thickness position. In the following a delamination is modelled as a 2 dimensional surface because it occurs between two plies in the laminate. The shape of the delamination is assumed circular with diameter  $s$ , see figure

2. The diameter  $s$  is modelled as a stochastic variable with an exponential distribution.

$$F_s(s) = 1 - \exp(-\chi_s s) \quad (1)$$

where

$\chi_s$  intensity parameter for diameter  $s$

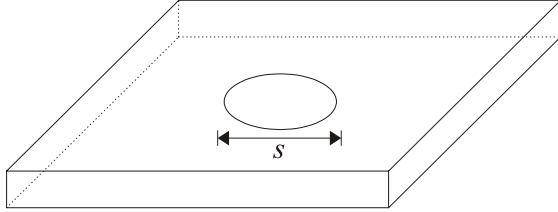


**Figure 2:** Planar circular delamination with diameter  $s$ .

### 3 Distribution of Defects

In the following section two models for the distribution of defects in wind turbine blades are proposed. The distribution of defects for the two models is illustrated by a numerical example with the main spar of a wind turbine blade.

#### 3.1 Model 1: Complete random distribution of defects

As previously stated, the position of defects in wind turbine blades has a significant influence on the reduction in load carrying capacity. In the present section a stochastic model for generation of completely random defects in a wind turbine blade is proposed in order to model the defects after production. Complete random defects will normally occur for a normal manufacturing process. The model assumes that the blade can be considered as a planar 2-dimensional region. Considering the blade as a planar region will for most defects be an appropriate assumption since defects tend to occur in a layer or in the interface between two layers of the laminate which leads to planar defects. The position of each planar defect in thickness can be modelled as a stochastic variable.

The distribution of defects on a planar region can be modelled by Complete Spatial Randomness (CSR) as described in [11] and [12]. The distribution of defects is based on two hypotheses:

i) The number of defects in the region  $A$  with area  $|A|$  follows a Poisson distribution.

ii) The distribution of the  $n$  events in the region  $A$  is an independent random sample from the uniform distribution on  $A$ .

The first hypothesis (i) gives the following Poisson distribution for the number of defects  $n$  in the region  $A$ .

$$P_{N|A}(n) = \frac{(\lambda |A|)^n \exp(-\lambda |A|)}{n!} \quad (2)$$

where  $n$  is the number of defects in the region  $A$ ,  $\lambda$  is the intensity parameter and  $|A|$  is the area of the region  $A$ .

The mean value  $\mu_N$  and variance  $\sigma_N^2$  for the number of defects in the region  $A$  are given by:

$$\mu_N = \lambda |A| \quad (3)$$

$$\sigma_N^2 = \lambda |A| \quad (4)$$

The intensity parameter  $\lambda$  is for CSR modelled as a constant in (2), (3) and (4) corresponding to a homogenous Poisson process. For real wind turbine blades the intensity parameter can vary with position on blade or size of the blade. Also, the time for manufacturing can influence the intensity parameter and lead to an inhomogenous Poisson process. However, wind turbine blade manufacturers monitor the manufacturing process in order to keep a constant quality of the blades. This monitoring will lead to a nearly constant intensity parameter and thereby a homogeneous Poisson process.

The second hypothesis (ii) specifies that the position of the individual defects should be sampled from a uniform distribution in the region  $A$ . The uniform distribution over a region can easily be obtained if the region is squared or rectangular. For more complex regions uniform distributed defects can be modelled by the following approach, see also figure 3 [13].

- 1) Define a squared or rectangular region  $A'$  for which  $A \subset A'$ .
- 2) Generate uniform distributed defects on  $A'$  until  $n$  defects are obtained in  $A$ .

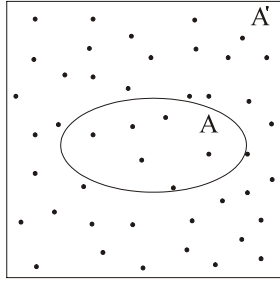


**Figure 3:** Uniform distribution of defect in the region  $A$ .

When the number of defects  $n$  in the region  $A$  is determined together with the position of the individual defect these defects can be attached additional discrete or continuous information.

Discrete information can e.g. be information about the type of defect or the shape of a defect. In order to model the discrete information stochastic a discrete probability distribution function must be specified for each parameter.

Continuous information can e.g. be information about the size of each defect. The continuous parameters are modelled by a continuous probability distribution function for each of the parameters. For delaminations (circle) the size is modelled by the diameter  $s$  which is considered as a stochastic variable.

### 3.2 Model 2: Random cluster distribution of defects

The model presented in section 3.1 was based on the assumption that defects occur randomly and independent which will be the case for a normal manufacturing process. However, if the manufacturing process is abnormal a defect in a wind turbine blade can trigger additional defects in the area close to the defect. In the following this effect is taken into account by using a clustered Poisson process, see [11] and [13].

The clustered Poisson distribution is based on a number of “parent” defects  $n_p$ . The parent defects are generated based on the model for complete spatial randomness given in section 3.1. For each of the parent defects a number of “offspring” defects are defined. Only the offspring defects represent the final distribution of defects. The distribution of random cluster defects is based on the following three hypotheses:

- i) The parent events form a complete random distribution, see section 3.1.
- ii) Each parent defect produces a number of offsprings  $n_o$  following a Poisson distribution.
- iii) The position of the offspring defects relative to their parent is independently and identically distributed according to a bivariate probability density function  $h$ .

The first hypothesis (i) gives the following homogeneous Poisson distribution for the number of parent defects  $n_p$  in the region  $A$ .

$$P_{N_p|A}(n_p) = \frac{(\kappa_p |A|)^{n_p} \exp(-\kappa_p |A|)}{n_p!} \quad (5)$$

where  $n_p$  is the number of parent defects in the region  $A$  and  $\kappa_p$  is the intensity parameter for the parent defect.

The hypothesis (ii) states, that also the number of offsprings from each parent defects follows a Poisson distribution given by:

$$P_{N_o}(n_o) = \frac{(\kappa_o)^{n_o} \exp(-\kappa_o)}{n_o!} \quad (6)$$

where  $n_o$  is the number of offsprings for each parent defect and  $\kappa_o$  is the intensity parameter for the offspring defects.

The last hypothesis (iii) specifies the position of the individual offsprings. In the following it is assumed that the distance from the parent defect to the offspring is given by a bivariate normal distribution which in general will lead to many offsprings located relatively close to the parent defect.

$$h(x_1, y_1) = \frac{1}{2\pi\sigma^2} \exp\left(-\frac{x_1^2 + y_1^2}{2\sigma^2}\right) \quad (7)$$

where  $x_1, y_1$  are the coordinates from parent defect to the offspring defect and  $\sigma$  is the standard deviation for the distance.

By modelling the position of the defects by a distance from the parent gives the disadvantage that the specified position of the defects can be located outside the region  $A$ .

In order to avoid this edge effect a periodic boundary condition is imposed [11].

- 1) Any generated  $x$ -coordinates of the form  $ka + x$ , for a non-zero integer  $k$  and  $0 < x < a$  is transformed to  $x$ .
- 2) Any generated  $y$ -coordinates of the form  $kb + y$ , for a non-zero integer  $k$  and  $0 < y < b$  is transformed to  $y$ .

The periodic boundary condition is specified for a planar rectangular region with length and width  $a, b$ . However, this assumption can to some extent be relaxed by use of the following substitutions  $a = a(y)$  and  $b = b(x)$ . The assumption of a periodic boundary condition will normally be a good approximation in the longitudinal direction of the blade.

The expected number of defects in the region  $A$  obtained by the clustered Poisson process is given by:

$$\mu_N = \kappa_o \kappa_p |A| \quad (8)$$

The variance for the number of defects can be calculated numerically.

### 3.3 Distribution of delaminations

In the following, a wind turbine blade which consists of a main spar and an aerodynamic shell, see figure 4, is used as a case study.

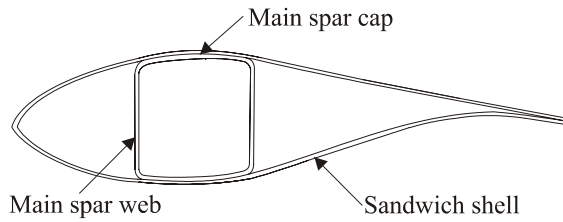


**Figure 4:** Cross section of blade profile.

The main purpose of the aerodynamic shell is to give the optimal aerodynamic shape of the blade and give support for loading in the edgewise direction. The aerodynamic shell is a sandwich structure with faces of laminated composite material. The main purpose of the spar is to carry loads in torsion and in the flapwise direction. The spar webs are also made of a sandwich structure with faces of biaxial laminas whereas the spar caps are made of unidirectional and biaxial laminas.

The main spar carries about 90% of the loads in the flapwise direction and is in the following considered alone for simplicity purpose. The approach taken is, however, general and could easily be extended to the entire blade.

For flapwise loading of the main spar the most probable failure modes are:

- Tensile failure in spar cap
- Compression failure in spar cap
- Buckling failure in spar cap
- Shear failure in spar webs
- Instability of the webs

The main spar can be considered as a planar region if the box is unfolded to a plate, see figure 5.

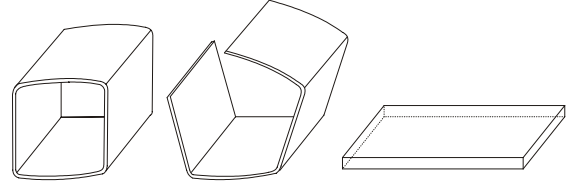


**Figure 5:** Planar representation of main spar.

When the main spar is unfolded to a plate an edge effect is introduced. In order to avoid this edge effect a periodic boundary condition is imposed in the longitudinal direction of the main spar, see section 3.2.

In figure 6 and figure 7 realisations of the position for delaminations in the main spar are given for model 1 (section 3.1) and model 2 (section 3.2).

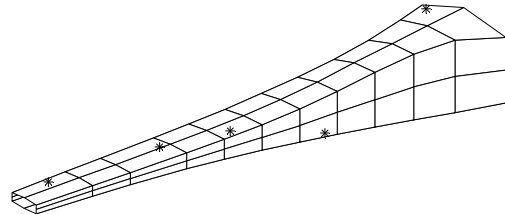


**Figure 6:** Realisations of defects model 1.

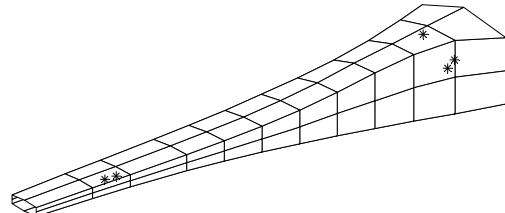


**Figure 7:** Realisations of defects model 2.

From figure 6 it is seen that the delaminations occur randomly in the blade. However, on



figure 7 the delaminations appear in clusters with typically 1-3 delaminations.

#### 4 Non Destructive Inspection

In the previous section the position, size and type of production defects have been modelled as stochastic variables. After manufacturing the wind turbine blade is normally quality controlled by Non Destructive Inspection (NDI) such as visual inspection or ultrasound scanning in order to detect larger defects in the blade.

The ability of these NDI-methods to indicate defects in the blade can be modelled by Probability of Detection (PoD) curves. The probability of detection will normally be dependent on the size and type of the defect. But also the through thickness position of the defects can have a significant influence on the probability of detection.

PoD-curves have previously been used for cracks in e.g. welded steel structures [14]. In composite materials and sandwich structures the methods for NDI have been considered in e.g. [6]. In the following, representative PoD-curves are modelled by an exponential distribution and depend only on the size of the defects.

$$F_{S_\delta}(\delta | s) = 1 - \exp(-\chi_{PoD}s) \quad (9)$$

where  $\delta$  is detection of a defect,  $S_\delta$  is the smallest detectable defect (stochastic) and  $\chi_{PoD}$  is the intensity parameter for delaminations.

Defects such as delaminations are normally rather easy to find by NDI-methods whereas for example wrinkles are much harder to find. This means that the intensity parameter should be dependent on the defect type. Using results from NDI the distribution of the defect size can be updated by Bayesian methods.

$$f_s(s | NDI) = \frac{f_{S_\delta}(\delta | s)f_s(s)}{\int_0^\infty f_{S_\delta}(\delta | s)f_s(s)ds} \quad (10)$$

where  $f_s(s | NDI)$  is the probability for delamination diameter  $s$  after NDI.

By inserting the prior distribution for the delamination size (1) and the likelihood

function for the probability of detection (9) in (10) the posterior distribution for the delamination size is given by:

$$f_s(s | NDI) = (\chi_s + \chi_{PoD}) \exp(-(\chi_s + \chi_{PoD})s) \quad (11)$$

with mean value and variance given by:

$$\mu_{s|NDI} = \frac{1}{\chi_s + \chi_{PoD}} \quad (12)$$

$$\sigma_{s|NDI}^2 = \frac{1}{(\chi_s + \chi_{PoD})^2} \quad (13)$$

In the present case the posterior distribution is also an exponential distribution since the exponential distribution is a conjugated prior to the likelihood function. For other choices of prior and likelihood function these will not necessarily be conjugated and the posterior distribution must then be calculated numerically.

In figure 8 the distribution functions for the delamination diameter are given after production and after NDI. The mean delamination size after production is assumed to be  $\mu_s = 0.20$  m and the mean size of delaminations detected by NDI is assumed to be  $\mu_{PoD} = 0.10$  m. The mean size of the delaminations after NDI is  $\mu_{s|NDI} = 0.07$  m.

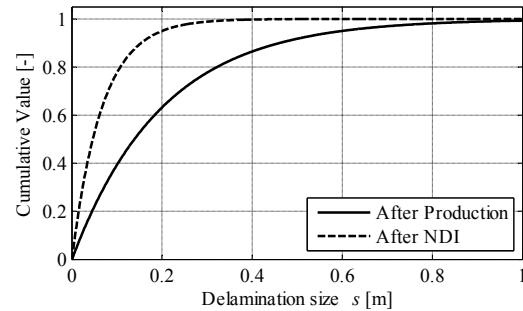


**Figure 8:** Distribution of delamination size.

If the defect growth is modelled by a stochastic model with more than one stochastic variable, then Bayesian methods can be used to model the inspection result, e.g. 'no-find' of a defect.

The Non Destructive Inspection methods are, however, not perfect, which leads to indication of defects even though there are no defects in the given area. This effect can be modelled by the Probability of False Indication (PFI), which is dependent on the area which is inspected [14].

## 5 Reliability Assessments

In this section methods for assessment of the probability of failure for wind turbine blades containing defects are studied. Failure due to damage accumulation (fatigue) is in the following neglected and only ultimate loading is considered. The methods are based on the models for distribution of defects presented in section 3.

### 5.1 General limit state function

In the general case the probability of failure in ultimate loading can be calculated from the limit state function:

$$g = X_R R(\sigma_{\max}, \epsilon_{\max}, \mathbf{E}, \mathbf{D}) - X_L L \quad (14)$$

where  $X_R$  is the model uncertainty for the capacity model  $R$ . The capacity model depends on  $\sigma_{\max}^T = \{X_c, X_t, Y_c, Y_t, S\}$  which is a vector containing the ultimate stress strength for the individual lamina.  $\epsilon_{\max}^T = \{\epsilon_{1c}, \epsilon_{1t}, \epsilon_{2c}, \epsilon_{2t}, \epsilon_6\}$  is a vector containing the ultimate strain strength for the individual lamina.  $\mathbf{E}^T = \{E_1, E_2, G_{12}, \nu_{12}\}$  is a vector containing the elastic properties for the individual lamina and the vector  $\mathbf{D}$  is containing information about the defects in the blade such as type, size, location and NDI.  $X_L$  is the model uncertainty for the load model  $L$  which among others depend on the mean wind speed, turbulence intensity and type / settings of the control system.

The stresses and strains in the wind turbine blade can be calculated based on nonlinear FE analysis. However, in order to determine the capacity  $R$ , a definition of failure must be established. For a perfect laminate failure of a ply/lamina can be determined based on one of several failure criteria [15].

- Maximum strain
- Maximum stress
- Tsai-Hill
- Tsai-Wu
- Puck

Also failure modes such as buckling related to local or global instability should be taken into account.

The definition of failure for the wind turbine blade is often in reliability calculations

determined from failure of the individual ply/lamina in one of the following ways:

- First Ply Failure (FPF)
- Last Ply Failure (LPF)

The wind turbine blade can for the FPF be interpreted as a series system of laminas and for the LPF as a parallel system. Defining failure of the wind turbine blade according to FPF will lead to an upper bound for the probability of failure and similar the LPF will lead to a lower bound. Wind turbine blades are normally designed in order to obtain damage tolerance of the blade for which reason the blade can be considered as a series system of parallel systems.

The limit state function (14) can unfortunately not be used directly to estimate the probability of failure. However, the probability of failure can be determined by either using simulation or by modifying the limit state function. In the following, the two approaches are elaborated.

### 5.2 Simulation

The probability of failure for a wind turbine blade containing defects can be determined by Monte Carlo simulation of the limit state function. By simulating input parameters which are used in a FE analysis, the failure criteria can be calculated and the probability of failure evaluated.

The input information about the defects in the wind turbine blade (number, type, size and location) is generated from one of the two stochastic models presented in section 3. For each realization the generated defects are implemented in the FE model together with realizations of the material properties. The material properties are the elastic properties  $\mathbf{E}$  and the ultimate strength stresses and strains  $\sigma_{\max}$  and  $\epsilon_{\max}$  which are modelled by random fields. Local strength reductions due to the generated defects should be modelled by a stochastic mode dependent on the defects type and size. Also realizations of the ultimate load should be generated after which the FE analysis can be performed. Based on the calculated stresses and strains the failure criteria can be checked and “failure” or “no failure” can be determined. From the Monte Carlo simulation the probability of failure can be determined by:



$$P_F = \frac{N_{failure}}{N_{sim}} \quad (15)$$

where  $N_{failure}$  is the number of simulations leading to failure and  $N_{sim}$  is the total number of simulations. However, in order to get a good approximation of  $P_F$  the total number of simulations has to be high which makes the simulation approach time consuming.

### 5.3 Modified limit state function

The limit state function (14) can be modified by explicitly taking the influence of the defects in the wind turbine blade into account.

For the wind turbine blade not containing any defects the ratio  $\alpha_{intact}$  can be defined as the factor by which the 50-year load distribution (characteristic load) can be increased before the blade fails using characteristic material properties. Similarly, the ratio  $\alpha_{defect}$  can be defined for the blade containing defects. If the structural model is linear, failure is determined by FPF and the same failure criteria is used in the code-based deterministic design then  $\alpha_{intact} = \gamma_m \gamma_n \gamma_f$ . The partial safety factors are given in [8] and listed in table 1.

**Table 1:** Partial safety factors [8].

Partial safety factor	Value
$\gamma_m$ - Material properties	1.3
$\gamma_n$ - Consequences of failure	1.0
$\gamma_f$ - Loads	1.35

The ratio between  $\alpha$  for the blade not containing defects and the blade containing defects are defined as the influence factor  $\theta$  which determines the influence of defects on the load carrying capacity.

$$\theta = \frac{\alpha_{defect}}{\alpha_{intact}} \quad (16)$$

From the ratio  $\alpha$  the modified limit state function can be formulated.

$$g(\alpha) = \frac{\alpha}{\alpha_{intact}} X_R R(\sigma_{max}, \epsilon_{max}, \mathbf{E}) - X_L L \quad (17)$$

where  $\sigma_{max}$ ,  $\epsilon_{max}$  and  $\mathbf{E}$  do not depend on the defects. The ratio  $\alpha$  depends on the number, type, size and location of the defects which can

be generated by the models presented in section 3. Also the uncertainty in the assessment of the strength reduction due to these defects is contained in  $\alpha$ . The probability of failure based on the modified limit state function can be calculated as.

$$P_F = \sum_{\alpha} P(g(\alpha) \leq 0) P(\alpha) \quad (18)$$

where  $P(g(\alpha) \leq 0)$  is the probability of failure given  $\alpha$  which can be calculated by the First Order Reliability Method (FORM) [16].  $P(\alpha)$  is the probability for getting the ratio  $\alpha$  and the summation over  $\alpha$  corresponds to summing over all numbers, types, sizes and positions of the defects. The reliability index  $\beta$  is defined based on the probability of failure.

$$\beta = -\Phi^{-1}(P_F) \quad (19)$$

## 6 Reliability of Main Spar

In the following section a numerical example with the reliability of the main spar in section 3.3 is considered. The probability of failure is determined using the modified limit state function in section 5.3. Failure of the individual ply/lamina is defined by the maximum strain criteria and failure of the spar is defined by First Ply Failure.

### 6.1 Load carrying capacity

The load carrying capacity is first calculated for the main spar not containing any defects. The strains in the spar during ultimate loading are calculated by a geometrical nonlinear FE analysis. The input parameters to the analysis are besides the geometry also material properties which can be either characteristic or design values. The load is applied at three sections in the longitudinal direction and scaled linearly until failure occurs. A part of the finite element model is shown in figure 9 for the load step corresponding to the characteristic load carrying capacity. From the figure it is seen that the pressure side of the main spar goes into a global buckling mode leading to high strains in the transverse direction. The high strains become critical because the cap is mainly made of unidirectional laminas.

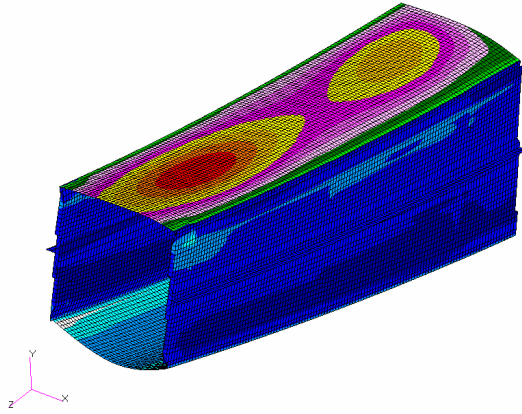


**Figure 9:** Global strains in x-direction (transverse) for the section from 9.6m to 12.1m from the root.

In figure 10, the strains in the transverse and longitudinal direction of the main spar are given dependent on the load level. The strains are plotted for the unidirectional lamina in the most critical position, which is located 11.7m from the root in the inner side of the main spar cap in compression. The strains are normalized with respect to the characteristic strain and the load is normalized with the characteristic load carrying capacity.

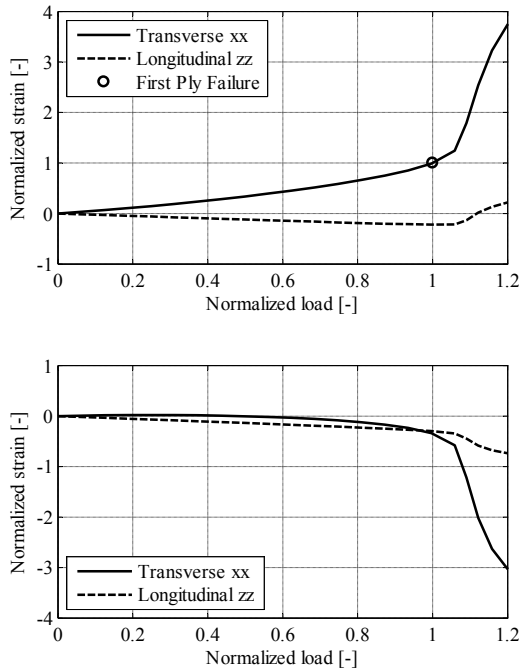


**Figure 10:** Normalized strains in transverse and longitudinal direction, unidirectional lamina. Top: inner side. Bottom: outer side.

From figure 10 (Top) it is seen that the strains in the transverse direction increase slightly

nonlinear until FPF after which the strains increase suddenly due to buckling of the main spar cap and collapse of the webs. In the longitudinal direction the cap is in compression until buckling where tension is developed in the inner side of the cap. The strains in the longitudinal direction are in general small compared to the characteristic value. The transverse strains in the outer side of the main spar, figure 10 (Bottom), are slightly smaller than in the inner side of the main spar cap. In the longitudinal direction the strains (compression) are higher than on the inner side.

Based on the finite element calculation for the main spar not containing any defects are  $\alpha_{\text{intact}}$  calculated to  $\alpha_{\text{intact}} = 1.53$ , which is lower than the product of the partial safety factors due to the nonlinear behaviour.

The strength reduction of the laminate due to a delamination is estimated based on representative tests. In the tests panels containing different sizes of delaminations are loaded in in-plane compression until failure and the strains in the longitudinal direction of the unidirectional fibers are measured. The strength reduction in the transverse direction is not tested. The through thickness position of the delaminations is 20% of the thickness and the size of the delaminations tested corresponds to 30 and 40% of the panel width. The compression strains in the longitudinal direction at failure are given in table 2 where the strains are normalized with respect to the mean strain at failure in case of no defects. The tests indicate a coefficient of variation for the results on approximately 10-20%.

**Table 2:** Mean compression strain in the longitudinal direction at failure for delaminations.

Defect	Size	Strain
No defect	-	1.00
Delamination	30%	0.63
-	40%	0.47
-	50%	0.32*

\* The value is estimated.

In the following it is assumed that a delamination with the same properties as tested is located at the most critical position in the main spar and having one of the following diameters:

- 30% of cap width -  $s = 0.19$  m
- 40% of cap width -  $s = 0.25$  m
- 50% of cap width -  $s = 0.31$  m

The load carrying capacity of the main spar is then determined using the reduced ultimate maximum strain estimated from table 2 for compression in the longitudinal direction. It is assumed that the width of the main spar cap can be regarded as width of the tested panels.

If the strength is only assumed to be reduced for compression in the longitudinal direction of the unidirectional fibers the delaminations will not influence the load carrying capacity. This is due to the low strength of the fibers in the transverse direction and that failure is determined by FPF. In the following it is assumed that the strength reduction in the transverse direction (tension) is 50% of the reduction for compression in the longitudinal direction given in table 2. The validity of this assumption has not been verified. The ratio  $\alpha$  and factor  $\theta$  are given in table 3 for the delamination in the main spar.

**Table 3:**  $\alpha$  and  $\theta$  values for main spar containing a defect.

Defect	Size	$\alpha_{\text{defect}}$	$\theta$
Delamination	30%	1.39	0.91
-	40%	1.31	0.86
-	50%	1.23	0.81

The factors  $\theta$  indicate that the characteristic load carrying capacity of the main spar is reduced 10-20% for the delaminations corresponding to 30-50% of the width for the main spar cap.

## 6.2 Sensitivity analysis

In order to determine the influence of the material properties on the load carrying capacity a sensitivity analysis is performed. The sensitivities are determined for the main spar not containing any defects and are performed for the three most important material properties which are assumed to be:

- Ultimate tensile strain transverse  $\varepsilon_{2t}$
- Longitudinal elasticity modulus  $E_1$
- Transverse elasticity modulus  $E_2$

The sensitivities are determined for the unidirectional laminas and no sensitivity analysis for the core material and biax laminas has been performed. The sensitivity analysis is performed by reducing the characteristic material properties 5% one by one and then recalculating the load carrying capacity. The calculated capacities are given in table 4 where all capacities have been normalized with

respect to the characteristic load carrying capacity.

**Table 4:** Sensitivity analysis for material properties.

Parameter	Load carrying capacity
Characteristic	1.000
$\varepsilon_{2t}$	0.980
$E_1$	0.984
$E_2$	0.985

From table 4 it is seen that the three parameters each decrease the characteristic load carrying capacity approximate 1-2% when they are reduced by 5%.

## 6.3 Reliability assessment

The probability of failure for the main spar can be determined from the modified limit state function given in section 5.3. The design equation for the blade in ultimate loading is given by:

$$G = \frac{z}{\gamma_n} R_d(\varepsilon_{2t}, E_1, E_2) - \gamma_f L_c \quad (20)$$

where  $z$  is a design parameter which balances the equation, index  $c$  is used for characteristic values, and index  $d$  is used for design values. The limit state function in ultimate loading is given by:

$$g(\alpha) = \frac{z\alpha}{\alpha_{\text{intact}}} X_R R(\varepsilon_{2t}, E_1, E_2) - X_L L \quad (21)$$

The capacity model  $R$  is determined by a linearization of the load carrying capacity for the characteristic material properties.

$$R = R_c + \sum_{i=1}^n (x_i - x_{ic}) \frac{\partial R_c}{\partial x_{ic}} \quad (22)$$

where  $x_i$  is the material property  $i$  and  $x_{ic}$  is the characteristic value for material property  $i$ .

The linearization is performed for the same material properties as the sensitivity analysis in section 6.2 and the other material properties are neglected. The stochastic models for the parameters in the limit state function is given in table 5 and are among others based on [17] and [18]. The individual material properties are assumed uncorrelated based on statistical assessment of the results from the Optimat Blades project [19].

**Table 5:** Stochastic models limit state function.

Variable	Distribution	COV
$\varepsilon_{2t}$	Lognormal	10 %
$E_1$	Lognormal	5 %
$E_2$	Lognormal	5 %
$X_R$	Lognormal	5 %
$X_L$	Lognormal	25 %
$L$	Gumbel	23 %

The probability of failure and the reliability index are given in table 6 for the main spar containing one delamination located at the most critical position. Three different sizes of delaminations are considered. It is assumed that the delamination gives a reduction in the ultimate transverse strain, see section 6.1.

After the production process the wind turbine blades are quality controlled by NDI as described in section 4. By assuming that the defects detected by the NDI are perfectly repaired the probability of failure can be updated dependent on the probability of detection. By assuming that the blade contains one defect the updated probability of failure is given by.

$$P_{F|defect,NDI} = P(g(\alpha_{intact}) \leq 0)P(\delta | NDI) + P(g(\alpha_{defect}) \leq 0)(1 - P(\delta | NDI)) \quad (23)$$

where the probability  $P(\delta | NDI)$  is the probability for detecting the defect by NDI. In case of several defects the updated probability of failure should be determined based on the different combinations of detection and no detection.

Assuming that the main spar is quality controlled by an NDI method as described in section 4 the updated probability of failure is calculated by (23) and given in table 6. It is assumed that the mean of the smallest detectable delamination corresponds to a diameter with  $\mu_{PoD} = 0.10$  m.

**Table 6:** Probability of failure and reliability index before and after NDI.

Defect	Size	$P_F$	$\beta$
No defect	-	$1.9 \cdot 10^{-3}$	2.90
Delamination	30%	$4.0 \cdot 10^{-3}$	2.65
-	40%	$6.2 \cdot 10^{-3}$	2.50
-	50%	$1.0 \cdot 10^{-2}$	2.33
Delamination   NDI	30%	$2.2 \cdot 10^{-3}$	2.85
-	40%	$2.2 \cdot 10^{-3}$	2.84
-	50%	$2.3 \cdot 10^{-3}$	2.84

From table 6 it is seen that the reliability index for the main spar not containing any defects is slightly lower than the target reliability index  $\beta = 3.09$  in [8]. The lower reliability index can be due to the nonlinear behaviour of the strains but also the failure criteria for the individual plies and the main spar can influence the result.

The delaminations located at the most critical position increase the probability of failure approximately by one order of magnitude. However, because the delaminations are rather large the probability of detection by NDI is high leading to a significant updating of the probability of failure. The updated probability of failure is based on the assumption that the delaminations are perfectly repaired.

## 7 Conclusion and future work

In this paper a framework for modelling of defects in wind turbine blades is presented - especially, the distribution of defects in wind turbine blades and the reliability of the blades in the ultimate limit state are considered.

For the distribution of defects two stochastic models are proposed. The defects are for the first model distributed completely random in the blade by a homogeneous Poisson process. For the second model the defects will tend to occur in clusters which are modelled by two coupled homogeneous Poisson processes.

The defects in the wind turbine blades are an outcome from the production process and will influence the reliability of the blade, dependent on their number, type, size and location. In a numerical example, the reliability for the main spar of a wind turbine blade is determined for three different sizes of defects in the shape of delaminations. The largest delamination increases the probability of failure with approximate one order of magnitude. Based on inspection of the main spar after production by NDI the probability of failure can be updated significantly.

The probability of failure in ultimate loading is mainly reduced by large delaminations which have a high probability of detection by the NDI. However, smaller delaminations which are much harder to detect can grow due to stress concentrations. This can have a significant influence on the fatigue and ultimate capacity later in the service life. This effect should be studied further. Also the influence of variations

in the material strength over the blade should be studied.

Reliability based inspection planning and risk based inspection planning have in several years been used to determine optimal inspection plans for welded joints in offshore steel structures. The methods presented in this paper can be used as a starting point for the development of similar inspection plans for wind turbine blades. This is especially relevant for fatigue loading where the defects can increase between the inspection intervals.

## Acknowledgement

The work presented in this paper is part of the project "Probabilistic design of wind turbines" supported by the Danish Research Agency, grant no. 2104-05-0075. The financial support is greatly appreciated.

The work is also partly supported by the Danish Energy Authority through the Energy Research Programme (EFP). The supported EFP-project is titled "Improved design of large wind turbine blades of fibre composites – phase 4" and has journal no. 33033-0267.

## References

- [1] Lekou DJ, Philippidis TP. Probabilistic Strength Assessment of FRP Laminates. 2007. Report No.: Upwind Deliverable 3.3.2.
- [2] Jolma P, Segercrantz S, Berggreen C. Ultimate failure of debond damaged sandwich panels loaded with lateral pressure - An experimental and fracture mechanics study. *Journal of Sandwich Structures & Materials* 2007 Mar;9(2):167-96.
- [3] Nokkentved A, Lundsgaard-Larsen C, Berggreen C. Non-uniform compressive strength of debonded sandwich panels - I. Experimental investigation. *Journal of Sandwich Structures & Materials* 2005 Nov;7(6):461-82.
- [4] Berggreen C, Simonsen BC. Non-uniform compressive strength of debonded sandwich panels - II. Fracture mechanics investigation. *Journal of Sandwich Structures & Materials* 2005 Nov;7(6):483-517.
- [5] Hayman B, Berggreen C, Pettersson R. The effect of face sheet wrinkle defects on the strength of FRP sandwich structures. *Journal of Sandwich Structures & Materials* 2007 Jul;9(4):377-404.
- [6] Hayman B. Approaches to damage assessment and damage tolerance for FRP sandwich structures. *Journal of Sandwich Structures & Materials* 2007 Nov;9(6):571-96.
- [7] ISO 2394. ISO - General Principles on Reliability of Structures. 1998.
- [8] IEC 61400-1. Wind turbines - Part1: Design requirements. 3<sup>rd</sup> edition. 2005.
- [9] Hayman B, Wedel-Heinen J, Brondsted P. Materials challenges in present and future wind energy. *Mrs Bulletin* 2008 Apr;33(4):343-53.
- [10] Short GJ, Guild FJ, Pavier MJ. The effect of delamination geometry on the compressive failure of composite laminates. *Composites Science and Technology* 2001;61(14):2075-86.
- [11] Diggle PJ. *Statistical Analysis of Spatial Point Patterns*. 2nd Edition ed. Arnold Publishers; 2003.
- [12] Veneziano D. *Random Processes for Engineering Applications*. (Lecture Notes) Massachusetts Institute of Technology; 1978.
- [13] Baddeley A. *Analysing spatial point patterns in R*. (Workshop Notes) CSIRO, Australia; 2008.
- [14] Straub D. *Generic Approaches to Risk Based Inspection Planning for Steel Structures* Swiss Federal Institute of Technology Zürich; 2004.
- [15] Soden PD, Kaddour AS, Hinton MJ. Recommendations for designers and researchers resulting from the world-wide failure exercise. *Composites Science and Technology* 2004 Mar;64(3-4):589-604.
- [16] Madsen HO, Krenk S, Lind NC. *Methods of Structural Safety*. Dover Publications, Inc.; 2006.
- [17] Lekou DJ, Philippidis TP. Mechanical property variability in FRP laminates and its effect on failure prediction. *Composites Part B-Engineering* 2008 Oct;39(7-8):1247-56.
- [18] Tarp-Johansen NJ, Madsen PH, Frandsen S. *Partial Safety Factors for Extreme Load Effects*. Risø National Laboratory, Roskilde, Denmark; 2002. Report No.: Risø-R-1319(EN).
- [19] OPTIMAT BLADES. 2006. <http://www.wmc.nl/>.